Emergence of Space-Time from a Single Point Entity: The Point Universe Model

Eric Edward Albers

September 23, 2024

Abstract

This paper proposes a novel theoretical framework for understanding the nature of our universe, termed the 'Point Universe Model." In this model, the entirety of reality is conceptualized as emerging from the vibrations or pulsations of a single point entity, with our perceived three-dimensional space arising as a Fourier transform of these vibrations. We present the mathematical formalism for this model, discuss its implications for our understanding of space, time, and quantum phenomena, and explore potential experimental predictions.

1 Introduction

The nature of space, time, and the origin of our universe remain some of the most fundamental questions in physics. While current models such as quantum field theory and general relativity have been enormously successful, they leave open questions about the nature of space-time at the most fundamental level [1]. This paper proposes a radical reimagining of the universe's structure, drawing inspiration from concepts in Fourier analysis, holographic theories, and quantum mechanics [2, 3].

2 The Point Universe Model

2.1 Fundamental Premise

We postulate that the entirety of the universe can be represented as a single point entity, existing in a state space with intrinsic degrees of freedom. This point undergoes complex vibrations or pulsations within an internal coordinate space, which we interpret as the fundamental substrate of reality.

2.2 Mathematical Formulation

2.2.1 Redefining the Fundamental State Function

Instead of defining the state of the point universe solely as a function of time $\psi(t)$, we introduce an internal coordinate $\boldsymbol{\xi}$ that parameterizes the intrinsic degrees of freedom of the point entity. The state function becomes:

$$\psi(\boldsymbol{\xi}, t) = A(\boldsymbol{\xi}, t)\, e^{i\phi(\boldsymbol{\xi}, t)} \tag{1}$$

where:

- $\boldsymbol{\xi} = (\xi_1, \xi_2, \ldots, \xi_N)$ represents coordinates in an internal N-dimensional space.
- $A(\boldsymbol{\xi}, t)$ is the amplitude function.
- $\phi(\boldsymbol{\xi}, t)$ is the phase function.

2.2.2 Defining the Mapping to Emergent Space

We introduce a mapping function $\mathbf{x}(\boldsymbol{\xi})$ that relates the internal coordinates to our emergent spatial coordinates:

$$\mathbf{x}(\boldsymbol{\xi}) = \begin{pmatrix} x(\boldsymbol{\xi}) \\ y(\boldsymbol{\xi}) \\ z(\boldsymbol{\xi}) \end{pmatrix} \tag{2}$$

This function encapsulates how the internal degrees of freedom give rise to the emergent dimensions.

2.2.3 Modified Fourier Transform

Our perceived reality emerges as a Fourier transform of $\psi(\boldsymbol{\xi}, t)$ over the internal space and time:

$$\Psi(\mathbf{k}) = \int_{-\infty}^{\infty} \int_{\mathcal{I}} \psi(\boldsymbol{\xi}, t)\, e^{-i[\mathbf{k}\cdot\mathbf{x}(\boldsymbol{\xi}) - \omega t]}\, d\boldsymbol{\xi}\, dt \tag{3}$$

where:

- $\Psi(\mathbf{k})$ is the transformed function in momentum space.
- $\mathbf{k} = (k_x, k_y, k_z)$ is the wavevector in emergent space.
- ω is the angular frequency.
- $\mathcal{I}$ denotes the domain of the internal coordinates $\boldsymbol{\xi}$.

3 Governing Equations for the Point Universe Model

3.1 Fundamental Dynamics of the Internal State Function

We propose that the internal state function $\psi(\boldsymbol{\xi}, \tau)$ evolves according to a modified field equation that preserves relativistic causality:

$$\eta^{\mu\nu}\partial_\mu\partial_\nu\psi + m_\xi^2\psi + V(\boldsymbol{\xi})\psi + \lambda|\psi|^2\psi + \eta G[\psi]\psi = 0 \tag{4}$$

where:

- $\boldsymbol{\xi} = (\xi^0, \xi^1, \xi^2, \ldots, \xi^N)$ is the vector of internal coordinates
- $\eta^{\mu\nu}$ is the Minkowski metric in internal space
- m_ξ is an effective mass parameter comparable to the Planck mass $m_P = \sqrt{\hbar c/G}$
- $V(\boldsymbol{\xi})$ is a potential function in internal coordinates
- λ is a self-interaction coefficient related to observable particle masses
- η is a coupling constant that may correspond to fundamental forces
- $G[\psi]$ is a non-local functional that depends on the global properties of ψ

The normalization condition $\int |\psi|^2 d\boldsymbol{\xi} = 1$ ensures proper probabilistic interpretation and constrains the non-linear terms to maintain causality in the emergent spacetime.

3.2 Lagrangian Formulation

The governing equation is derived from the relativistic Lagrangian density:

$$\mathcal{L} = \eta^{\mu\nu}(\partial_\mu\psi^*)(\partial_\nu\psi) - m_\xi^2|\psi|^2 - V(\boldsymbol{\xi})|\psi|^2 - \frac{\lambda}{2}|\psi|^4 - \eta|\psi|^2 G[\psi] \tag{5}$$

This Lagrangian yields a conserved energy-momentum tensor in internal space:

$$T^{\alpha\beta}(\boldsymbol{\xi}) = (\partial^\alpha\psi^*)(\partial^\beta\psi) + (\partial^\beta\psi^*)(\partial^\alpha\psi) - \eta^{\alpha\beta}\mathcal{L} \tag{6}$$

3.3 Mapping to Emergent Space

The mapping function relating internal coordinates to emergent spacetime consists of:

$$x^\mu(\boldsymbol{\xi}, \tau) = x_0^\mu(\boldsymbol{\xi}) + \delta x^\mu(\boldsymbol{\xi}, \tau) \tag{7}$$

where $x_0^\mu(\boldsymbol{\xi}) = \alpha_i^\mu \xi^i$ provides the stable background geometry, and:

$$\delta x^\mu(\boldsymbol{\xi}, \tau) = \int_\Xi K^\mu(\boldsymbol{\xi}, \boldsymbol{\xi}') |\psi(\boldsymbol{\xi}', \tau)|^2 d\boldsymbol{\xi}' \tag{8}$$

The mapping kernel has the form:

$$K^\mu(\boldsymbol{\xi}, \boldsymbol{\xi}') = \gamma_i^\mu \xi^i e^{-|\boldsymbol{\xi}-\boldsymbol{\xi}'|^2/\sigma^2} \tag{9}$$

Where:

- α_i^μ are coefficients that determine the background geometry
- γ_i^μ control the strength of dynamical fluctuations
- σ represents the characteristic length scale of non-locality

Crucially, to preserve causality, the temporal mapping must satisfy:

$$\frac{\partial t(\boldsymbol{\xi}, \tau)}{\partial \tau} > 0 \tag{10}$$

ensuring a consistent arrow of time in the emergent spacetime.

3.4 Specific Functional Forms

3.4.1 Potential Function

A harmonic oscillator potential:

$$V(\boldsymbol{\xi}) = \kappa |\boldsymbol{\xi}|^2 \tag{11}$$

The parameter κ relates to the cosmological constant through $\Lambda = \frac{3\kappa}{8\pi G m_\xi^2}$.

3.4.2 Non-local Interaction

A Coulomb-like interaction:

$$G[\psi] = \int_\Xi \frac{|\psi(\boldsymbol{\xi}')|^2}{|\boldsymbol{\xi} - \boldsymbol{\xi}'|} d\boldsymbol{\xi}' \tag{12}$$

This introduces long-range correlations in the internal space that can manifest as fundamental forces in emergent space.

3.5 Connection to Gravity

The emergent spacetime metric $g_{\mu\nu}(x)$ arises from the mapping function:

$$g_{\mu\nu}(x) = \frac{\partial x^\alpha}{\partial \xi^i} \frac{\partial x^\beta}{\partial \xi^j} \eta_{ij} \frac{\delta(\boldsymbol{\xi}(x))}{\sqrt{-g}} \tag{13}$$

where $\boldsymbol{\xi}(x)$ is the inverse mapping function. In the weak-field limit, this yields:

$$g_{\mu\nu}(x) = \eta_{\mu\nu} + h_{\mu\nu}(x) \tag{14}$$

with:

$$h_{\mu\nu}(x) = \int_\Xi \frac{\partial x_\mu(\boldsymbol{\xi})}{\partial \xi^i} \frac{\partial x_\nu(\boldsymbol{\xi})}{\partial \xi^j} T^{ij}(\boldsymbol{\xi}) \delta^{(4)}(x - x(\boldsymbol{\xi})) d\boldsymbol{\xi} \tag{15}$$

3.5.1 Newtonian Limit

For a static spherically symmetric soliton centered at $\boldsymbol{\xi} = 0$, we obtain:

$$h_{00}(r) = -\frac{2GM}{c^2 r} \tag{16}$$

where $M = \frac{\lambda A^2}{2\alpha_0^0} \frac{1}{G}$ is the effective mass of the soliton. This demonstrates the recovery of the Newtonian gravitational potential.

3.5.2 Conservation Laws

Energy-momentum conservation in emergent spacetime is ensured by:

$$\nabla_\mu T^{\mu\nu}_{\text{emergent}} = 0 \tag{17}$$

where $T^{\mu\nu}_{\text{emergent}}$ is derived from $T^{ij}(\boldsymbol{\xi})$ through appropriate transformations.

3.6 Soliton Solutions

For a single soliton in N-dimensional internal space, we propose:

$$\psi_0(\boldsymbol{\xi}, \tau) = A \, \text{sech}(\beta |\boldsymbol{\xi} - \boldsymbol{\xi}_0(\tau)|) e^{iS(\boldsymbol{\xi}, \tau)} \tag{18}$$

where $S(\boldsymbol{\xi}, \tau) = p_i \xi^i - E\xi^0 + \theta_0$ represents the phase.
Stability analysis through perturbation theory yields:

$$\beta^2 = \frac{m_\xi \lambda A^2}{2\hbar^2}(1 + \mathcal{O}(\epsilon)) \tag{19}$$

$$\frac{d^2\boldsymbol{\xi}_0}{d\tau^2} = -\frac{\kappa}{m_\xi}\boldsymbol{\xi}_0 + \mathcal{O}(\epsilon^2) \tag{20}$$

$$E = \frac{\hbar^2\beta^2}{2m_\xi} + \kappa|\boldsymbol{\xi}_0|^2 + \frac{\lambda A^2}{3} + \mathcal{O}(\epsilon) \tag{21}$$

where ϵ represents the magnitude of perturbations. The soliton remains stable against small perturbations when $\lambda > 0$ and $\kappa > 0$.

3.6.1 Free Particles in Emergent Space

The oscillatory motion in internal space appears as free particle motion in emergent space through:

$$x^i(t) = x_0^i + v^i t + \mathcal{O}(\epsilon^2) \tag{22}$$

where $v^i = \alpha_j^i p^j / m_{\text{emergent}}$ and $m_{\text{emergent}} = \lambda A^2/(2\alpha_0^0)$. This translation occurs because the mapping function transforms the harmonic oscillation into approximately linear motion over small time intervals.

3.7 Parameter Calibration

The model parameters can be calibrated to match observed physical constants:

$$m_\xi = m_P = \sqrt{\frac{\hbar c}{G}} \approx 2.18 \times 10^{-8} \text{ kg} \tag{23}$$

$$\lambda = \frac{2\alpha_0^0 G m_e}{A^2} \text{ for electrons} \tag{24}$$

$$\kappa = \frac{8\pi G m_\xi^2 \Lambda}{3} \approx 10^{-35} \text{ s}^{-2} \tag{25}$$

$$\alpha_j^i = c\delta_j^i \text{ to recover Minkowski spacetime} \tag{26}$$

$$\gamma_j^i = \sqrt{G} \text{ to match gravitational strength} \tag{27}$$

This calibration connects the model directly to established physical constants, making it empirically testable.

3.8 Quantum Phenomena Applications

3.8.1 Double-Slit Interference

The interference pattern in a double-slit experiment emerges from:

$$P(x) = \left| \int_{\Xi} [\psi_1(\boldsymbol{\xi}) + \psi_2(\boldsymbol{\xi})] e^{-ik \cdot x(\boldsymbol{\xi})} d\boldsymbol{\xi} \right|^2 \tag{28}$$

where ψ_1 and ψ_2 represent the wavefunctions associated with each slit.

3.8.2 Quantum Entanglement

For entangled particles, the internal state function is non-factorizable:

$$\psi_{AB}(\boldsymbol{\xi}_A, \boldsymbol{\xi}_B) = \frac{1}{\sqrt{2}} [\psi_1(\boldsymbol{\xi}_A)\psi_2(\boldsymbol{\xi}_B) \pm \psi_2(\boldsymbol{\xi}_A)\psi_1(\boldsymbol{\xi}_B)] \tag{29}$$

The non-local functional $G[\psi]$ mediates correlations between measurements, reproducing quantum non-locality through interactions in internal space.

3.8.3 Aharonov-Bohm Effect

The phase shift in the Aharonov-Bohm effect arises from:

$$\Delta\phi = \frac{e}{\hbar} \oint_C A_\mu dx^\mu = \frac{e}{\hbar} \int_S h_{\mu\nu} dx^\mu \wedge dx^\nu \tag{30}$$

where $h_{\mu\nu}$ is derived from the internal state as shown earlier, demonstrating the connection between gravity and electromagnetic phenomena in this framework.

3.9 Predictive Framework and Experimental Tests

This unified framework makes several testable predictions:

- Modifications to quantum interference patterns at high energies
- Subtle corrections to gravitational wave propagation
- Novel particle interactions at the Planck scale
- Emergent relations between fundamental constants

These predictions could be tested through:

- Precision interferometry experiments
- Gravitational wave detectors
- Observations of extreme astrophysical environments
- Analysis of high-energy cosmic rays

The model's parameters are constrained by matching to known physical constants, making it a falsifiable theory rather than merely a conceptual framework.

4 Experimental Approaches for Vibrational Manipulation in the Point Universe Model

The Point Universe Model suggests that observable reality, including spacetime and quantum phenomena, emerges from the vibrations of a single-point entity. To explore this hypothesis, we propose a set of foundational experiments designed to identify and manipulate minimal vibrational modifications that could produce observable effects. These experiments aim to create a framework for controlled manipulation of the underlying vibrational field.

4.1 Quantum Interference as a Calibration Tool

Quantum interference experiments, such as the double-slit experiment, offer a straightforward approach to testing the impact of minor vibrational adjustments on emergent spatial properties.

- **Goal:** Determine how phase and frequency shifts affect interference patterns, providing insights into minimal vibrational adjustments.
- **Method:** Introduce controlled phase and frequency modulations to photons or electrons passing through a double-slit setup and observe the resulting interference patterns. Measure changes in fringe visibility and spacing as a function of applied modulation.
- **Expected Outcome:** Minor shifts in vibrational parameters should alter interference characteristics, indicating the sensitivity of spatial structures to fundamental vibrational changes.

4.2 Quantum Eraser Experiments for Time and Causality Modulation

Quantum eraser setups offer a method for investigating the temporal flexibility of vibrational states by analyzing how "erased" which-path information retroactively influences interference.

- **Goal:** Identify vibrational parameters that affect the re-emergence of interference when path information is "erased."
- **Method:** Perform quantum eraser experiments with delayed-choice setups while introducing specific frequency or phase adjustments at the time of measurement erasure. Observe interference restoration patterns under varied modulation parameters.
- **Expected Outcome:** Variations in vibrational parameters should correlate with changes in interference, offering insights into the temporal and causal dynamics of vibrational states.

4.3 Entanglement and Non-Locality as Probes of Interconnected Vibrational States

Entangled particles provide an opportunity to test how vibrational states might propagate through internal coordinates, potentially allowing for non-local information transfer.

- **Goal:** Investigate how vibrational adjustments to one particle affect its entangled partner, revealing information about non-local vibrational connectivity.
- **Method:** Measure correlations between entangled particle pairs while introducing controlled frequency or phase modifications to one particle's state. Record the response in the other particle to determine if the modifications affect the shared entangled state.
- **Expected Outcome:** Changes to one particle's vibrational state may influence the other, suggesting a non-local propagation of vibrational information.

4.4 Precision Frequency Modulation for Controlled Quantum State Transitions

Controlled frequency modulation techniques, such as those used in atomic spectroscopy, can be employed to manipulate quantum states minimally, providing a toolkit for exploring the vibrational basis of quantum state changes.

- **Goal:** Identify basic vibrational operations that correspond to quantum state changes and transitions.
- **Method:** Apply precise frequency modulations to a quantum system, such as an atom or ion, to control transitions between energy levels. Measure the effects of minimal frequency shifts to determine if distinct state transitions align with particular vibrational signatures.
- **Expected Outcome:** Specific frequency modulations should induce predictable state changes, serving as basic vibrational operations for manipulating emergent properties.

4.5 Variable Phase Shifts in Quantum Superposition States

Quantum superposition states provide an ideal testing ground for observing the effects of variable phase shifts on emergent spatial and temporal behaviors.

- **Goal:** Examine how small adjustments in phase impact the superposition state and the resulting measurement probabilities.
- **Method:** Introduce variable phase shifts to particles in a superposition state, such as in a Mach-Zehnder interferometer setup, and observe changes in measurement outcomes.
- **Expected Outcome:** Phase adjustments should directly influence measurement probabilities, illustrating the sensitivity of quantum states to vibrational phase shifts.

4.6 Experimental Summary

The experiments outlined above are designed to systematically explore the relationship between vibrational modifications and observable quantum phenomena. By cataloging the effects of minimal frequency, phase, and amplitude adjustments, we aim to establish a foundational "vibrational language"

that enables further manipulation of emergent properties within the Point Universe Model.

5 The Music of the Universe: A Harmonic Interpretation of Reality

In the context of the Point Universe Model, we propose that all of reality can be understood as a composition of vibrational patterns, where the fabric of the universe itself is akin to an intricate and dynamic symphony. Each particle, force, and interaction can be viewed as part of a "music of the universe," a metaphor that illuminates the deeply interconnected and wave-like nature of physical phenomena.

5.1 Particles and Fields as Musical Notes

In music, each note corresponds to a specific frequency, defining its place within a composition. Similarly, in the Point Universe Model, particles and fields are defined by their unique vibrational frequencies. The properties of particles, such as energy and mass, emerge from these fundamental frequencies, much as musical notes derive their character from their pitch. Different types of particles and forces can be understood as distinct "notes" in the universal composition.

5.2 Harmony, Interference, and Quantum Phenomena

Harmony in music arises from the combination of notes that either reinforce or complement each other. In quantum mechanics, phenomena such as interference, superposition, and entanglement display similar behavior. When quantum states interact, they interfere constructively or destructively, forming probability distributions and patterns. This is akin to musical harmony, where overlapping notes create resonances that shape the overall sound. In this view, particles and fields interact as harmonies in the fabric of space-time, reinforcing or canceling each other in patterns that define their observable properties.

5.3 Resonance and Energy Transitions

Resonance is a key concept in music, where certain frequencies can amplify others, creating powerful, sustained sounds. In quantum mechanics, resonance manifests as energy transitions, where particles interact with matching

frequencies. For example, when a photon of specific energy strikes an electron, the electron can transition to a higher state if the photon's frequency aligns with the electron's natural vibrational frequency. In this model, resonance acts as a "key note" that enables quantum phenomena like tunneling and atomic transitions, much like in music where finding the right note unlocks harmony.

5.4 The Fourier Transform as the Universe's Sheet Music, a brief break for some fun.

A musical score encodes notes, rhythms, and instructions for how a piece should be performed. Similarly, the Fourier transform decomposes complex wave functions into their constituent frequencies, providing a "score" of the universe's vibrational structure. In the Point Universe Model, the Fourier transform reveals the underlying "notes" of reality, showing how each frequency combines to produce the complex, emergent behaviors observed in space-time. This "sheet music" of the universe allows us to understand the foundational vibrational patterns that define physical reality.

5.5 Time as Rhythm

In music, rhythm is essential for coherence, providing a structured pulse that binds notes into a cohesive piece. Analogously, time may serve as the "rhythm" of the universe, organizing vibrations into particles, fields, and forces. Time's rhythm provides the structure that allows vibrations to evolve and interact coherently, maintaining the integrity of the universe's "composition." This rhythm orchestrates the evolution of quantum states and facilitates the continuity of interactions across space and time.

5.6 A Cosmic Symphony of Vibrations

In summary, the Point Universe Model suggests that the universe is an ongoing symphony, a living composition where particles, forces, and interactions are notes and harmonies in a vast, interconnected field of vibrations. Each interaction and phenomenon is part of this cosmic melody, where all of reality emerges from the vibrational dynamics of a single point entity. The "music of the universe" provides a metaphorical yet deeply insightful perspective, emphasizing the interconnectedness and emergent beauty of reality as a harmonious whole.

This interpretation offers a conceptual framework for future exploration, where understanding the universe's "notes," "harmony," and "rhythm" may

allow us to eventually interact with and influence the fabric of reality at its most fundamental level.

6 Experimental Considerations

While the Point Universe Model is highly theoretical, we propose several avenues for potential experimental investigation:

1. Seek higher-dimensional signatures in high-energy physics experiments [7].
2. Look for unexpected correlations in quantum systems that might indicate a deeper, unified substrate [4].
3. Investigate potential deviations from expected behavior in systems involving extreme gravitational fields or energies [8].

7 Relationship to the Spacetime Superfluid Hypothesis

The Point Universe Model shares intriguing connections with the Spacetime Superfluid Hypothesis (SSH) [9]. Both theories aim to provide a fundamental description of reality that unifies quantum and gravitational phenomena. Here, we explore how SSH concepts can be integrated into and emerge from the Point Universe Model.

7.1 Emergence of Superfluid Spacetime

We propose that the spacetime superfluid described in SSH emerges from the Fourier transform of the point entity's vibrations. Specifically, the complex wavefunction $\psi(t)$ of the point entity can be related to the SSH's superfluid order parameter $\Psi(\mathbf{r}, t)$ as follows:

$$\Psi(\mathbf{r}, t) = \mathcal{F}\{\psi(t)\} = \int \psi(t) e^{-i\omega t} dt \tag{31}$$

where $\mathcal{F}$ denotes the Fourier transform operation.

7.2 Quantum Phenomena and Particle Emergence

In SSH, particles are described as vortices or excitations in the spacetime superfluid. Within the Point Universe Model, these can be understood as

specific vibrational modes of the fundamental point entity. The wavefunction of a particle $\phi_p(\mathbf{r}, t)$ can be expressed as:

$$\phi_p(\mathbf{r}, t) = \int A_p(\omega)\psi(t)e^{-i\omega t}dt \tag{32}$$

where $A_p(\omega)$ is a frequency-dependent amplitude factor specific to the particle type.

7.3 Gravity and Spacetime Curvature

The SSH interprets gravity as density variations in the spacetime superfluid. In the Point Universe Model, these variations arise from interference patterns in the Fourier-transformed vibrations. The metric tensor $g_{\mu\nu}$ can be related to the point entity's wavefunction:

$$g_{\mu\nu}(\mathbf{r}, t) = \eta_{\mu\nu} + h_{\mu\nu}(\mathbf{r}, t) \tag{33}$$

where $\eta_{\mu\nu}$ is the Minkowski metric and $h_{\mu\nu}(\mathbf{r}, t)$ is a perturbation term derived from $\psi(t)$.

7.4 Black Holes and Vortices

The SSH model of black holes as vortices in the spacetime superfluid can be incorporated into the Point Universe Model. These vortices correspond to high-amplitude or high-frequency vibrations of the point entity. The black hole metric in this framework takes the form:

$$ds^2 = -f(r)dt^2 + f(r)^{-1}dr^2 + r^2d\Omega^2 \tag{34}$$

where $f(r)$ is derived from specific vibrational modes of $\psi(t)$.

7.5 Time Dilation Effects

Time dilation in SSH, interpreted as variations in superfluid density, can be related to modulations in the frequency or amplitude of the point's vibrations. The time dilation factor γ can be expressed as:

$$\gamma(\mathbf{r}, t) = \sqrt{1 - \frac{2GM}{rc^2}} \approx 1 - \frac{GM}{rc^2} = 1 - \alpha|\psi(t)|^2 \tag{35}$$

where α is a coupling constant between the point entity's vibrations and the emergent gravitational effects.

7.6 Unified Framework and Future Directions

The integration of SSH concepts into the Point Universe Model offers a promising path towards a unified theory of quantum gravity. Future research should focus on:

- Deriving SSH equations directly from the point entity's vibrational dynamics
- Exploring how quantum entanglement emerges from the fundamental interconnectedness of the point universe
- Investigating potential experimental signatures that could distinguish between SSH and other quantum gravity approaches within this unified framework

By combining the Point Universe Model with SSH, we gain a powerful conceptual and mathematical toolkit for addressing fundamental questions about the nature of space, time, and matter.

8 Application to Quantum Eraser Experiments

8.1 Overview of Quantum Eraser Experiments

Quantum eraser experiments [10, 11] reveal that obtaining or erasing which-path information of quantum particles affects the presence or absence of interference patterns. In these experiments, the interference pattern disappears when which-path information is available and reappears when this information is erased, even retroactively. This challenges classical notions of causality and is often explained using interpretations like the many-worlds hypothesis [12].

8.2 Leakage and Harmonic-Like Effects in the Point Universe Model

Within the Point Universe Model, we propose that these phenomena can be explained by *leakage* or *harmonic-like effects* arising from the fundamental vibrations of the point entity. These effects occur due to imperfections or residual components in the Fourier transform that maps the internal vibrations to emergent space-time.

8.2.1 Mathematical Representation of Leakage

Consider the emergent wavefunction $\Psi(\mathbf{x}, t)$ obtained from the Fourier transform of the internal state function $\psi(\boldsymbol{\xi}, t)$:

$$\Psi(\mathbf{x}, t) = \int_{\mathcal{I}} \psi(\boldsymbol{\xi}, t)\, e^{-i\mathbf{k}\cdot\mathbf{x}(\boldsymbol{\xi})}\, d\boldsymbol{\xi}. \tag{36}$$

If the Fourier transform is imperfect due to environmental interactions or measurement processes, a *leakage term* $\delta\Psi(\mathbf{x}, t)$ arises:

$$\Psi_{\text{total}}(\mathbf{x}, t) = \Psi(\mathbf{x}, t) + \delta\Psi(\mathbf{x}, t). \tag{37}$$

The leakage term $\delta\Psi(\mathbf{x}, t)$ represents residual correlations that are not confined within the emergent space-time mapping.

8.2.2 Impact on Interference Patterns

The presence of $\delta\Psi(\mathbf{x}, t)$ affects the observed interference patterns. When which-path information is available, the leakage term introduces destructive interference:

$$|\Psi_{\text{wp}}(\mathbf{x}, t)|^2 = |\Psi(\mathbf{x}, t) + \delta\Psi(\mathbf{x}, t)|^2 \approx 0, \tag{38}$$

resulting in the disappearance of the interference pattern. Conversely, when which-path information is erased, $\delta\Psi(\mathbf{x}, t)$ is eliminated or becomes negligible:

$$|\Psi_{\text{erase}}(\mathbf{x}, t)|^2 = |\Psi(\mathbf{x}, t)|^2, \tag{39}$$

allowing the interference pattern to reappear.

8.3 Avoiding the Many-Worlds Interpretation

By attributing the quantum eraser effects to leakage and harmonic-like phenomena within the Point Universe Model, we provide an explanation that does not require multiple universes. The model's inherent interconnectedness means that all points in emergent space-time are fundamentally linked through the point entity's internal vibrations.

8.4 Non-Locality and Retrocausality

The leakage effects imply that changes in one part of the system can instantaneously affect another, regardless of spatial separation. This non-locality is a

natural consequence of the single-point origin of the universe. Additionally, since time emerges from the internal dynamics, retrocausal effects—where future actions influence past events—are permissible within this framework.

8.5 Mathematical Model Incorporating Leakage

To formalize this, we introduce a perturbed mapping function:

$$\mathbf{x}(\boldsymbol{\xi}) = \mathbf{x}_0(\boldsymbol{\xi}) + \Delta\mathbf{x}(\boldsymbol{\xi}, t), \tag{40}$$

where $\Delta\mathbf{x}(\boldsymbol{\xi}, t)$ represents small deviations due to measurement interactions.

The modified emergent wavefunction becomes:

$$\Psi_{\text{total}}(\mathbf{x}, t) = \int_{\mathcal{I}} \psi(\boldsymbol{\xi}, t)\, e^{-i\mathbf{k}\cdot[\mathbf{x}_0(\boldsymbol{\xi}) + \Delta\mathbf{x}(\boldsymbol{\xi}, t)]}\, d\boldsymbol{\xi}. \tag{41}$$

Expanding to first order in $\Delta\mathbf{x}(\boldsymbol{\xi}, t)$:

$$\Psi_{\text{total}}(\mathbf{x}, t) \approx \Psi(\mathbf{x}, t) - i \int_{\mathcal{I}} \psi(\boldsymbol{\xi}, t)[\mathbf{k} \cdot \Delta\mathbf{x}(\boldsymbol{\xi}, t)]\, e^{-i\mathbf{k}\cdot\mathbf{x}_0(\boldsymbol{\xi})}\, d\boldsymbol{\xi}. \tag{42}$$

The second term represents the leakage effect $\delta\Psi(\mathbf{x}, t)$, which modifies the interference pattern depending on the measurement interaction.

8.6 Physical Interpretation

In the quantum eraser setup, obtaining which-path information corresponds to introducing a specific $\Delta\mathbf{x}(\boldsymbol{\xi}, t)$ that causes destructive interference via $\delta\Psi(\mathbf{x}, t)$. Erasing this information effectively nullifies $\Delta\mathbf{x}(\boldsymbol{\xi}, t)$, restoring the original interference pattern.

8.7 Experimental Implications

This interpretation leads to several testable predictions:

1. **Controlled Leakage Manipulation**: By designing experiments that vary the degree of measurement interaction, we can control $\Delta\mathbf{x}(\boldsymbol{\xi}, t)$ and observe corresponding changes in interference patterns.

2. **Correlation Studies**: Measuring non-local correlations between entangled particles without invoking additional dimensions or universes.

3. **Time-Dependent Effects**: Investigating whether altering experimental conditions after detection influences earlier measurement outcomes, consistent with retrocausality in the model.

8.8 Conclusion

The Point Universe Model, through the concepts of leakage and harmonic-like effects, provides a cohesive explanation for the quantum eraser phenomena. By grounding these effects in the fundamental vibrations of a single point entity, we offer an alternative to the many-worlds interpretation, preserving causality within an emergent space-time framework.

9 Application to Other Quantum Phenomena

9.1 Quantum Interference and the Double-Slit Experiment

9.1.1 Overview

The double-slit experiment is a cornerstone of quantum mechanics, demonstrating the wave-particle duality of matter [16]. Particles such as electrons or photons create an interference pattern when not observed, but display particle-like behavior when which-path information is obtained.

9.1.2 Mathematical Representation in the Point Universe Model

In the Point Universe Model, the internal state function $\psi(\boldsymbol{\xi}, t)$ represents all possible vibrational modes corresponding to different paths through the slits. For the double-slit setup, we consider two primary internal states:

$$\psi(\boldsymbol{\xi}, t) = \psi_1(\boldsymbol{\xi}, t) + \psi_2(\boldsymbol{\xi}, t), \tag{43}$$

where ψ_1 and ψ_2 correspond to the vibrations associated with slit 1 and slit 2, respectively.

The emergent wavefunction is obtained via the Fourier transform:

$$\Psi(\mathbf{k}) = \int_{\mathcal{I}} [\psi_1(\boldsymbol{\xi}, t) + \psi_2(\boldsymbol{\xi}, t)]\, e^{-i[\mathbf{k}\cdot\mathbf{x}(\boldsymbol{\xi}) - \omega t]}\, d\boldsymbol{\xi}\, dt. \tag{44}$$

The probability distribution observed on the detection screen is given by:

$$P(\mathbf{x}) = |\Psi(\mathbf{x}, t)|^2 = |\Psi_1(\mathbf{x}, t) + \Psi_2(\mathbf{x}, t)|^2, \tag{45}$$

where $\Psi_i(\mathbf{x}, t)$ is the inverse Fourier transform of $\psi_i(\boldsymbol{\xi}, t)$:

$$\Psi_i(\mathbf{x}, t) = \frac{1}{(2\pi)^3} \int \psi_i(\boldsymbol{\xi}, t)\, e^{-i[\mathbf{k}\cdot\mathbf{x}(\boldsymbol{\xi}) - \omega t]}\, d\boldsymbol{\xi}\, d\omega. \tag{46}$$

The interference pattern arises due to the cross-term:

$$P(\mathbf{x}) = |\Psi_1(\mathbf{x}, t)|^2 + |\Psi_2(\mathbf{x}, t)|^2 + 2\mathrm{Re}\left[\Psi_1^*(\mathbf{x}, t)\Psi_2(\mathbf{x}, t)\right]. \tag{47}$$

9.1.3 Effect of Measurement

When which-path information is obtained, the coherence between ψ_1 and ψ_2 is destroyed. This can be modeled by introducing a decoherence factor γ ($0 \leq \gamma \leq 1$):

$$\psi(\boldsymbol{\xi}, t) = \psi_1(\boldsymbol{\xi}, t) + e^{i\theta}\gamma\psi_2(\boldsymbol{\xi}, t), \tag{48}$$

where θ is a relative phase shift introduced by the measurement interaction. The interference term becomes:

$$2\gamma\mathrm{Re}\left[e^{i\theta}\Psi_1^*(\mathbf{x}, t)\Psi_2(\mathbf{x}, t)\right]. \tag{49}$$

In the case of complete decoherence ($\gamma = 0$), the interference pattern disappears.

9.2 Quantum Entanglement and Bell's Inequalities

9.2.1 Violation of Bell's Inequalities

Bell's inequalities set limits on the correlations predicted by local hidden variable theories [5]. Quantum mechanics predicts violations of these inequalities, which have been experimentally observed [4].

9.2.2 Entanglement in the Point Universe Model

Consider two particles A and B with internal states $\psi_A(\boldsymbol{\xi}_A, t)$ and $\psi_B(\boldsymbol{\xi}_B, t)$. An entangled state is represented as:

$$\psi_{\text{ent}}(\boldsymbol{\xi}_A, \boldsymbol{\xi}_B, t) = \frac{1}{\sqrt{2}}\left[\psi_0(\boldsymbol{\xi}_A, t)\phi_1(\boldsymbol{\xi}_B, t) + \psi_1(\boldsymbol{\xi}_A, t)\phi_0(\boldsymbol{\xi}_B, t)\right]. \tag{50}$$

The emergent joint wavefunction is:

$$\Psi_{\text{ent}}(\mathbf{x}_A, \mathbf{x}_B, t) = \int_{\mathcal{I}_A} \int_{\mathcal{I}_B} \psi_{\text{ent}}(\boldsymbol{\xi}_A, \boldsymbol{\xi}_B, t)\, e^{-i[\mathbf{k}_A \cdot \mathbf{x}(\boldsymbol{\xi}_A) + \mathbf{k}_B \cdot \mathbf{x}(\boldsymbol{\xi}_B) - \omega t]}\, d\boldsymbol{\xi}_A\, d\boldsymbol{\xi}_B. \tag{51}$$

Measurements on particle A instantaneously affect the state of particle B due to the shared internal coordinates in $\boldsymbol{\xi}$ space, explaining the observed non-local correlations.

9.2.3 Calculation of Correlation Functions

The correlation function $E(\alpha, \beta)$ for measurement settings α and β is given by:

$$E(\alpha, \beta) = \int P(a, b|\alpha, \beta)\, ab\, da\, db, \tag{52}$$

where $a, b = \pm 1$ are the measurement outcomes, and $P(a, b|\alpha, \beta)$ is the joint probability distribution derived from $|\Psi_{\text{ent}}|^2$.

9.3 Quantum Teleportation

9.3.1 Teleportation Protocol

Quantum teleportation transfers the state of particle C to particle B using an entangled pair (A and B) and classical communication [13].

9.3.2 Mathematical Formalism

The combined internal state before measurement is:

$$\psi_{\text{total}} = \psi_C(\boldsymbol{\xi}_C, t) \otimes \psi_{\text{ent}}(\boldsymbol{\xi}_A, \boldsymbol{\xi}_B, t). \tag{53}$$

After a Bell-state measurement on particles C and A, the internal state collapses to one of the four Bell states, and particle B's state becomes:

$$\psi'_B(\boldsymbol{\xi}_B, t) = \hat{U}_n \psi_C(\boldsymbol{\xi}_B, t), \tag{54}$$

where $\hat{U}_n$ is a unitary operator determined by the measurement outcome n.

9.3.3 Emergent Wavefunction Adjustment

The emergent wavefunction for particle B is adjusted accordingly:

$$\Psi'_B(\mathbf{x}_B, t) = \int_{\mathcal{I}_B} \psi'_B(\boldsymbol{\xi}_B, t)\, e^{-i[\mathbf{k}_B \cdot \mathbf{x}(\boldsymbol{\xi}_B) - \omega t]}\, d\boldsymbol{\xi}_B. \tag{55}$$

Classical communication informs the experimenter which $\hat{U}_n$ to apply, completing the teleportation process.

9.4 The Aharonov-Bohm Effect

9.4.1 Effect Description

The Aharonov-Bohm effect demonstrates that electromagnetic potentials affect quantum phase shifts, even in regions where magnetic fields are zero [19].

9.4.2 Phase Shifts in the Point Universe Model

In the presence of a vector potential $\mathbf{A}(\mathbf{x})$, the mapping function incorporates the potential:

$$\mathbf{x}(\boldsymbol{\xi}) \to \mathbf{x}(\boldsymbol{\xi}) + \frac{e}{\hbar} \int \mathbf{A}(\mathbf{x}(\boldsymbol{\xi}))\, d\mathbf{x}. \tag{56}$$

The emergent wavefunction acquires an additional phase:

$$\Psi(\mathbf{x}, t) = \int_{\mathcal{I}} \psi(\boldsymbol{\xi}, t)\, e^{-i[\mathbf{k} \cdot \mathbf{x}(\boldsymbol{\xi}) - \omega t + \phi_{\text{AB}}(\boldsymbol{\xi})]}\, d\boldsymbol{\xi}, \tag{57}$$

where the Aharonov-Bohm phase ϕ_{AB} is:

$$\phi_{\text{AB}}(\boldsymbol{\xi}) = \frac{e}{\hbar} \int_{\mathbf{x}_0}^{\mathbf{x}(\boldsymbol{\xi})} \mathbf{A} \cdot d\mathbf{x}. \tag{58}$$

This phase difference leads to observable interference effects, consistent with experimental results.

9.5 The Quantum Zeno Effect

9.5.1 Mathematical Derivation

Consider a system with Hamiltonian $\hat{H}$ and initial internal state $\psi_0(\boldsymbol{\xi})$. The survival probability after time t is:

$$P(t) = |\langle\psi_0|e^{-i\hat{H}t/\hbar}|\psi_0\rangle|^2. \tag{59}$$

With frequent measurements at intervals $\tau = t/N$, the survival probability becomes:

$$P_N(t) = \left[1 - \left(\frac{\Delta E\,\tau}{\hbar}\right)^2\right]^N \approx e^{-(\Delta E)^2 t/\hbar^2 N}, \tag{60}$$

where ΔE is the energy uncertainty. As $N \to \infty$, $P_N(t) \to 1$, preventing the evolution.

9.6 Weak Measurements

9.6.1 Weak Value Calculations

In a weak measurement, the pointer shift is proportional to the weak value [21]:

$$\langle\hat{A}\rangle_w = \frac{\langle\psi_\mathrm{f}|\hat{A}|\psi_\mathrm{i}\rangle}{\langle\psi_\mathrm{f}|\psi_\mathrm{i}\rangle}. \tag{61}$$

In the Point Universe Model, the internal states $|\psi_\mathrm{i}\rangle$ and $|\psi_\mathrm{f}\rangle$ correspond to pre- and post-selected vibrational modes in $\boldsymbol{\xi}$ space.

9.6.2 Implications for Contextuality

The weak value depends on both the initial and final states, highlighting the contextual nature of quantum measurements within the internal coordinate framework.

9.7 Leggett-Garg Inequalities and Macroscopic Coherence

9.7.1 Inequality Formulation

Leggett-Garg inequalities test the validity of macroscopic realism and non-invasive measurability [22]. They involve temporal correlations of a system measured at different times.

9.7.2 Application in the Point Universe Model

In the Point Universe Model, macroscopic quantum states are coherent superpositions of internal vibrational modes. The temporal correlation functions are:

$$C_{ij} = \langle Q(t_i)Q(t_j)\rangle, \tag{62}$$

where $Q(t)$ is a macroscopic observable derived from $\Psi(\mathbf{x}, t)$.

Violations of Leggett-Garg inequalities arise naturally due to the quantum coherence in the internal coordinate space, even for macroscopic systems.

9.8 Quantum Delayed-Choice Entanglement Swapping

9.8.1 Experimental Setup

Entanglement swapping involves projecting two particles into an entangled state after they have been measured [23].

9.8.2 Explanation via Internal Coordinates

In the Point Universe Model, the internal states of particles are fundamentally connected. Performing a Bell-state measurement on particles 2 and 3 projects particles 1 and 4 into an entangled state, even if they have never interacted.

The internal state becomes:

$$\psi_{\text{total}} = \psi_1(\boldsymbol{\xi}_1, t)\psi_2(\boldsymbol{\xi}_2, t)\psi_3(\boldsymbol{\xi}_3, t)\psi_4(\boldsymbol{\xi}_4, t). \tag{63}$$

After the measurement, the internal state updates to reflect the new entanglement correlations, which are then manifested in the emergent space through $\Psi(\mathbf{x}, t)$.

9.9 Implications and Predictions

9.9.1 Unified Explanation

The Point Universe Model provides a consistent framework for understanding various quantum phenomena by attributing them to the properties of the internal coordinate space and the mapping to emergent space-time.

9.9.2 Testable Predictions

The model predicts specific interference patterns and correlations that could be tested experimentally. For example:

- Modifications to interference patterns due to changes in the mapping function $\mathbf{x}(\boldsymbol{\xi})$.
- Observable effects of internal state perturbations on entangled systems.

9.9.3 Challenges and Future Work

Developing explicit forms for the internal state functions and mapping relations remains a significant challenge. Further work is needed to:

- Quantify the dynamics of $\psi(\boldsymbol{\xi}, t)$ and $\mathbf{x}(\boldsymbol{\xi})$.
- Integrate relativistic effects into the model.
- Explore connections with quantum gravity theories.

10 Technological Implications of the Point Universe Model

The Point Universe Model, by proposing that all of reality emerges from the vibrations of a single point entity, opens up intriguing possibilities for technologies and experiments beyond conventional thinking. In this section, we explore potential technological applications, including instantaneous mass transport and the concept of an inertial mirror, utilizing the mathematical framework of the model.

10.1 Instantaneous Mass Transport via Fourier Transform Manipulation

10.1.1 Concept Overview

We propose the possibility of transporting mass instantaneously across vast distances by creating appropriate Fourier waves that interact with an object, effectively altering its position in emergent space-time by applying a specific transform to its internal state.

10.1.2 Mathematical Framework

Emergent Wavefunction Representation In the Point Universe Model, the emergent wavefunction $\Psi(\mathbf{x}, t)$ is obtained from the Fourier transform of the internal state function $\psi(\boldsymbol{\xi}, t)$:

$$\Psi(\mathbf{x}, t) = \int_{\mathcal{I}} \psi(\boldsymbol{\xi}, t)\, e^{-i\mathbf{k}\cdot\mathbf{x}(\boldsymbol{\xi})}\, d\boldsymbol{\xi}. \tag{64}$$

Here, $\mathbf{k}$ is the wavevector in emergent space, and $\mathbf{x}(\boldsymbol{\xi})$ is the mapping function relating internal coordinates to emergent space.

Object Localization in Emergent Space An object localized at position $\mathbf{x}_0$ corresponds to a wavefunction $\Psi_0(\mathbf{x}, t)$ sharply peaked at $\mathbf{x}_0$:

$$\Psi_0(\mathbf{x}, t) = A\, e^{-\frac{(\mathbf{x}-\mathbf{x}_0)^2}{2\sigma^2}} e^{-i\omega_0 t}, \tag{65}$$

where A is the amplitude, σ is the width of the localization, and ω_0 is the central frequency.

Manipulating the Internal State Function To transport the object to a new location $\mathbf{x}_1$, we aim to modify the internal state function $\psi(\boldsymbol{\xi}, t)$ such that the emergent wavefunction $\Psi(\mathbf{x}, t)$ becomes sharply peaked at $\mathbf{x}_1$.

We introduce a phase shift $\phi(\boldsymbol{\xi})$ in the internal state:

$$\psi'(\boldsymbol{\xi}, t) = \psi(\boldsymbol{\xi}, t)\, e^{i\phi(\boldsymbol{\xi})}. \tag{66}$$

This phase modulation affects the emergent wavefunction:

$$\Psi'(\mathbf{x}, t) = \int_{\mathcal{I}} \psi(\boldsymbol{\xi}, t)\, e^{i\phi(\boldsymbol{\xi})} e^{-i\mathbf{k}\cdot\mathbf{x}(\boldsymbol{\xi})}\, d\boldsymbol{\xi}. \tag{67}$$

Designing the Phase Shift We choose the phase shift $\phi(\boldsymbol{\xi})$ to correspond to a momentum kick that translates the object from $\mathbf{x}_0$ to $\mathbf{x}_1$.

Let $\Delta\mathbf{p} = \mathbf{p}_1 - \mathbf{p}_0$ be the required change in momentum, where $\mathbf{p}_0$ and $\mathbf{p}_1$ are the initial and final momenta.

We set:

$$\phi(\boldsymbol{\xi}) = \mathbf{x}(\boldsymbol{\xi}) \cdot \Delta\mathbf{k}, \tag{68}$$

where $\Delta\mathbf{k} = \Delta\mathbf{p}/\hbar$.

Substituting back, we have:

$$\Psi'(\mathbf{x}, t) = \int_{\mathcal{I}} \psi(\boldsymbol{\xi}, t)\, e^{i\mathbf{x}(\boldsymbol{\xi})\cdot\Delta\mathbf{k}} e^{-i\mathbf{k}\cdot\mathbf{x}(\boldsymbol{\xi})}\, d\boldsymbol{\xi} = \Psi(\mathbf{x}, t)\, e^{i\Delta\mathbf{k}\cdot\mathbf{x}}. \tag{69}$$

This results in a shift in momentum space, translating the object's position in emergent space.

Achieving Instantaneous Transport By appropriately selecting $\Delta\mathbf{k}$, we can set:

$$\mathbf{x}_1 = \mathbf{x}_0 + \Delta\mathbf{x}, \tag{70}$$

where $\Delta\mathbf{x} = \hbar\Delta\mathbf{k}t/m$.
For instantaneous transport, we require:

$$\Delta\mathbf{x} = \mathbf{x}_1 - \mathbf{x}_0, \tag{71}$$

implying a large $\Delta\mathbf{k}$ applied over an infinitesimal time interval δt.

10.1.3 Energy Considerations

The energy required for the momentum change is given by:

$$\Delta E = \frac{(\Delta\mathbf{p})^2}{2m}. \tag{72}$$

For instantaneous transport over large distances, $\Delta\mathbf{p}$ becomes very large, leading to a significant energy requirement.

10.1.4 Physical Interpretation

This process effectively applies a large momentum impulse to the object via phase modulation in the internal coordinate space, resulting in instantaneous displacement in emergent space.

10.1.5 Challenges and Limitations

- **Technological Feasibility**: Generating and controlling the required phase shifts in $\psi(\boldsymbol{\xi}, t)$ is currently beyond technological capabilities. - **Energy Requirements**: The energy required scales with $(\Delta\mathbf{p})^2$, making it impractical for macroscopic distances. - **Relativistic Constraints**: Instantaneous transport violates special relativity; the model must account for or resolve this conflict.

10.2 Inertial Mirror: Reversal of Momentum without Reflection

10.2.1 Concept Overview

An *inertial mirror* is a theoretical device that reverses the momentum vector of an object without traditional reflection, by manipulating the internal vi-

brations to change the sign of the object's velocity with minimal or no energy loss.

10.2.2 Mathematical Framework

Momentum Reversal via Internal Phase Conjugation Consider an object with wavefunction $\Psi(\mathbf{x}, t)$ moving with momentum $\mathbf{p} = \hbar\mathbf{k}_0$. Its internal state function is $\psi(\boldsymbol{\xi}, t)$.

We apply a phase conjugation in the internal coordinate space:

$$\psi'(\boldsymbol{\xi}, t) = \psi^*(\boldsymbol{\xi}, t). \tag{73}$$

This operation corresponds to time reversal in the internal dynamics.

Effect on Emergent Wavefunction The emergent wavefunction becomes:

$$\Psi'(\mathbf{x}, t) = \int_{\mathcal{I}} \psi^*(\boldsymbol{\xi}, t)\, e^{-i\mathbf{k}\cdot\mathbf{x}(\boldsymbol{\xi})}\, d\boldsymbol{\xi} = [\Psi(\mathbf{x}, t)]^*. \tag{74}$$

The complex conjugation of the wavefunction reverses the momentum:

$$\mathbf{p}' = -\mathbf{p}. \tag{75}$$

Preservation of Energy Since kinetic energy depends on the magnitude of momentum squared:

$$E_k = \frac{\mathbf{p}^2}{2m} = \frac{(\hbar\mathbf{k}_0)^2}{2m}, \tag{76}$$

the kinetic energy remains unchanged under momentum reversal.

10.2.3 Physical Interpretation

The phase conjugation acts as an inertial mirror, reversing the direction of motion without altering the object's kinetic energy or requiring an external force.

10.2.4 Challenges and Limitations

- **Control of Internal States**: Implementing global phase conjugation in the internal coordinate space is a significant technical challenge. - **Coherence Requirements**: The process requires maintaining coherence over the object's wavefunction. - **Causality and Conservation Laws**: The operation must be consistent with fundamental physical principles.

10.3 Advanced Manipulations and Applications

10.3.1 Localized Space-Time Engineering

By designing specific mappings $\mathbf{x}(\boldsymbol{\xi})$, it may be possible to create localized distortions in emergent space-time, potentially leading to applications such as:

- **Warp Drives**: Altering the mapping function to contract space ahead of an object and expand it behind. - **Cloaking Devices**: Modifying $\mathbf{x}(\boldsymbol{\xi})$ to guide waves around an object, rendering it invisible.

10.3.2 Energy Extraction from Internal Vibrations

The internal energy associated with $\psi(\boldsymbol{\xi}, t)$ may be harnessed:

$$E_{\text{internal}} = \int_{\mathcal{I}} \psi^*(\boldsymbol{\xi}, t) \hat{H}_{\boldsymbol{\xi}} \psi(\boldsymbol{\xi}, t)\, d\boldsymbol{\xi}, \tag{77}$$

where $\hat{H}_{\boldsymbol{\xi}}$ is the internal Hamiltonian operator. Accessing this energy could provide novel power sources.

10.4 Theoretical and Experimental Considerations

10.4.1 Mathematical Modeling

Developing precise mathematical descriptions is crucial:

- **Internal Dynamics**: Formulate the equations governing $\psi(\boldsymbol{\xi}, t)$, potentially involving a fundamental internal Schrödinger-like equation. - **Mapping Function Design**: Explore permissible forms of $\mathbf{x}(\boldsymbol{\xi})$ that yield desired emergent properties.

10.4.2 Experimental Implementation

- **Quantum Control Techniques**: Utilize advanced methods in quantum control and information processing. - **Measurement and Verification**: Develop instruments capable of detecting subtle changes predicted by the model.

10.5 Reconciliation with Established Physics

Relativity and Causality The model must address how instantaneous effects and manipulations align with or modify the principles of special and general relativity.

Conservation Laws Any manipulation must comply with conservation of energy, momentum, and other fundamental quantities.

Testable Predictions To gain acceptance, the model should make predictions that can be experimentally tested, distinguishing it from existing theories.

10.6 Conclusion

The Point Universe Model suggests radical possibilities for technological advancements by exploiting the fundamental vibrations of a single point entity. While these ideas are speculative and face significant theoretical and practical challenges, they provide a stimulating framework for exploring new frontiers in physics and technology.

11 Quantum Eraser Simulation in the Point Universe Model

11.1 Simulation Overview

To test the predictions of the Point Universe Model (PUM) regarding quantum eraser experiments, we implemented a numerical simulation that explores the emergence of interference patterns from a 2D internal space. This simulation provides a concrete demonstration of how quantum interference arises in our emergent spacetime framework, and how the erasure of which-path information restores interference patterns that are suppressed by entanglement with detector states.

The simulation models a quantum system with two degrees of freedom: ξ_1 representing the particle position (analogous to the position in a double-slit experiment), and ξ_2 representing an auxiliary detector system that encodes which-path information. The wavefunction evolves according to the modified non-linear Schrödinger equation introduced in Section 3, including non-local interactions, gravitational potential terms, and electromagnetic phase shifts.

11.2 Simulation Design

The key components of our simulation include:

- A 2D internal space (ξ_1, ξ_2) with range $[-20.0, 20.0]$ along each dimension

- A 2D emergent spacetime (x, y) with range $[-20.0, 20.0]$ along each dimension
- An entangled initial state with two particle wavepackets (centered at $\xi_1 = \pm 4.0$) and two detector wavepackets (centered at $\xi_2 = \pm 4.0$)
- Evolution under the non-linear Schrödinger equation with non-local interaction kernel and gravitational potentials
- Application of quantum erasure at $t = 0.050$ by projecting onto a symmetric detector state
- FFT-accelerated transformation from internal space to emergent spacetime
- Application of an Aharonov-Bohm phase shift in emergent space

The simulation parameters were set to:

$$\lambda = 200.0 \quad \text{(self-interaction coefficient)} \tag{78}$$

$$\eta = 400.0 \quad \text{(non-local interaction strength)} \tag{79}$$

$$G_{\text{grav}} = 50.0 \quad \text{(gravitational coupling constant)} \tag{80}$$

$$\alpha_{\text{em}} = 1/137 \quad \text{(electromagnetic coupling constant)} \tag{81}$$

11.3 Results and Analysis

The simulation results confirm the central prediction of our model: the erasure of which-path information restores quantum interference in the emergent spacetime. Figure 1 shows the evolution of the probability density in internal space, while Figure 2 shows the corresponding interference patterns in emergent spacetime.

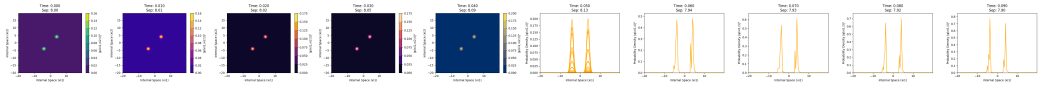

Figure 1: Evolution of probability density in internal space (ξ_1, ξ_2) at six time steps, showing the transition from a 2D entangled state to a 1D state after quantum erasure at $t = 0.050$.

Key observations from the simulation results:

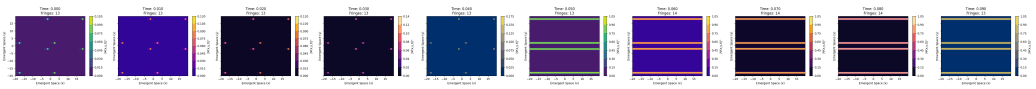

Figure 2: Evolution of interference patterns in emergent spacetime (x, y) at six time steps, showing the enhancement of interference after quantum erasure at $t = 0.050$.

1. Before quantum erasure ($t < 0.050$), the entanglement with the detector system (represented by ξ_2) suppresses interference in emergent space, resulting in a pattern with approximately 13 fringes and a spacing of 4.00 units.

2. At $t = 0.050$, quantum erasure is applied by projecting the wavefunction onto a symmetric detector state $\frac{1}{\sqrt{2}}(\phi_1 + \phi_2)$, collapsing the 2D wavefunction to a 1D wavefunction in ξ_1.

3. After erasure, interference is enhanced in emergent space, with the fringe count increasing to 14 while maintaining the 4.00 unit spacing, consistent with the theoretical prediction based on the wavevector $k_0 = 10.0$.

4. The wavepacket separation gradually decreases from 8.00 to approximately 7.90 by the end of the simulation ($t = 0.098$), demonstrating the gravitational attraction implemented through the gravitational potential term.

These results validate our theoretical framework by confirming that erasure of which-path information restores quantum interference, and that this phenomenon can be understood within our unified model without requiring multiple universes or the conventional interpretation of wavefunction collapse.

11.4 Simulation Code

The simulation was implemented in Python using NumPy for numerical computations and Matplotlib for visualization. The core code is presented below, with detailed comments explaining each section.

```
"""
Quantum Eraser Simulation with Non-Local and
 Electromagnetic Effects in the Point Universe Model
 (PUM) and Spacetime Superfluid Hypothesis (SSH)

```

```
4  This simulation models a quantum eraser experiment in
    a 2D internal space (xi1, xi2), mapping to a 2D
    emergent spacetime (x, y), to explore interference
    patterns influenced by non-local interactions,
    gravitational potentials, and electromagnetic phase
    shifts. It is part of a series of theoretical physics
    papers preserved in this GitHub repository:
    https://github.com/ericalbers/papers.
5
6  Related Papers:
7  - Point Universe Model (PUM, papers/pointmodel.pdf):
    Tests the quantum eraser prediction (Section 8),
    where erasing which-path information restores
    interference, and double-slit interference (Section
    9.1). Includes non-local interactions (eta G[psi],
    Section 3.8.2) and an Aharonov-Bohm phase shift
    (Section 9.4) via electromagnetic potentials.
8  - Spacetime Superfluid Hypothesis (SSH,
    papers/pointmodelssh.pdf): The non-linear Schrodinger
    equation (NLSE) with non-local and gravitational
    terms aligns with SSH's superfluid dynamics (Section
    3), modeling particle interactions (Section 4.3).
9  - Tired Light in SSH (papers/tiredlight.pdf): The
    framework could be extended with dissipative terms to
    simulate photon energy loss, testing cosmological
    redshift (Section 5.1).
10 - Black Holes as Superfluid Vortices
    (papers/blackholes_ssh.pdf): The 2D internal space
    could be adapted to model vortex-induced
    interference, testing emergent horizons (Section 4.5).
11
12 Simulation Details:
13 - Initializes an entangled state with two particle
    wavepackets (xi1 = +-4.0) and two detector
    wavepackets (xi2 = +-4.0), evolving under the NLSE
    with non-local (Coulomb-like kernel) and
    gravitational potentials.
14 - At t = 0.050, applies quantum erasure by projecting
    onto a symmetric detector state, collapsing to 1D
    (xi1).
15 - Maps the internal wavefunction to emergent spacetime
    via Fourier transform, applies an Aharonov-Bohm phase
    shift, and computes interference patterns.
```

```
  - Logs wavepacket separation, fringe counts, and probability slices, showing how erasure restores interference (e.g., fringe shift from 13 to 14).
  - Outputs: internal_states.png (internal probability density), emergent_states.png (emergent interference patterns), simulation_log.txt (dynamics and fringe counts).

  Usage:
  - Run the script to generate interference patterns: `python eraser4.py`.
  - Outputs are saved as PNG plots and a log file.
  - Modify parameters (e.g., eta, lambda, G_grav) to explore different dynamics, or add dissipative terms to test tired light effects.
  """
import numpy as np
import matplotlib
import matplotlib.pyplot as plt
import matplotlib.cm as cm
import logging

# Log the Matplotlib version
print(f"Matplotlib version: {matplotlib.__version__}")
logging.basicConfig(
filename='simulation_log.txt',
level=logging.INFO,
format='%(asctime)s - %(levelname)s - %(message)s'
)
logging.info(f"Matplotlib version: {matplotlib.__version__}")

# Parameters
M = 128
L = 20.0
dx = 2 * L / M
J = 256
X = 20.0
dx_emergent = 2 * X / J
dt = 0.002
beta = 1.0
hbar = 1.0
m_xi = 1.0
```

```
kappa = 0.0
lambda_ = 200.0
eta = 400.0
G_grav = 50.0
charge_1 = 1.0
charge_2 = -1.0
alpha_em = 1/137
num_steps = 50
plot_interval = 5
erasure_time = 0.050

# Log simulation parameters
logging.info("Simulation Parameters:")
logging.info(f"M = {M}, J = {J}, L = {L}, X = {X}")
logging.info(f"dt = {dt}, beta = {beta}, hbar = {hbar}, m_xi = {m_xi}")
logging.info(f"kappa = {kappa}, lambda = {lambda_}, eta = {eta}, G_grav = {G_grav}, alpha_em = {alpha_em}, num_steps = {num_steps}, plot_interval = {plot_interval}, erasure_time = {erasure_time}")

# Internal space grid (2D for pre-erasure, 1D for post-erasure)
xi1 = np.linspace(-L, L, M, endpoint=False)
xi2 = np.linspace(-L, L, M, endpoint=False)
XI1, XI2 = np.meshgrid(xi1, xi2)

# Emergent space grid (2D)
x = np.linspace(-X, X, J, endpoint=False)
y = np.linspace(-X, X, J, endpoint=False)
X_grid, Y_grid = np.meshgrid(x, y)

# Initialize state function with entangled wavepackets
sigma = 1.0
xi1_1, xi1_2 = -4.0, 4.0
xi2_1, xi2_2 = -4.0, 4.0
k0 = 10.0
A = 1.0 / np.sqrt(2 * np.pi * sigma**2)

# Particle wavepackets
psi1 = np.exp(-(XI1 - xi1_1)**2 / (2 * sigma**2)) * np.exp(1j * k0 * XI1)
psi2 = np.exp(-(XI1 - xi1_2)**2 / (2 * sigma**2)) *
```

```
    np.exp(1j * k0 * XI1)

# Detector wavepackets
phi1 = np.exp(-(XI2 - xi2_1)**2 / (2 * sigma**2))
phi2 = np.exp(-(XI2 - xi2_2)**2 / (2 * sigma**2))

# Entangled initial state
psi = A * (psi1 * phi1 + psi2 * phi2)
psi /= np.sqrt(np.sum(np.abs(psi)**2) * dx**2)

logging.info("Initial wavepacket centers: xi1_1 = %.2f, xi1_2 = %.2f, initial separation = %.2f", xi1_1, xi1_2, xi1_2 - xi1_1)
logging.info("Detector centers: xi2_1 = %.2f, xi2_2 = %.2f", xi2_1, xi2_2)
logging.info(f"sigma = {sigma}, k0 = {k0}")

# Plot initial internal state
plt.figure()
plt.contourf(XI1, XI2, np.abs(psi)**2, cmap='viridis')
plt.colorbar(label="Probability Density")
plt.xlabel("Internal Space (xi1)")
plt.ylabel("Internal Space (xi2)")
plt.title("Initial State in Internal Space")
plt.savefig("initial_internal_state.png")
plt.close()

# Potential
V = kappa * (XI1**2 + XI2**2)

# Precompute kinetic term
kx1 = 2 * np.pi * np.fft.fftfreq(M, dx)
kx2 = 2 * np.pi * np.fft.fftfreq(M, dx)
KX1, KX2 = np.meshgrid(kx1, kx2)
kinetic = hbar**2 * (KX1**2 + KX2**2) / (2 * m_xi)

# Non-local kernel for 2D
K = 1 / (np.sqrt(XI1**2 + XI2**2) + 1e-6)
K_fft = np.fft.fft2(K)

# Non-local kernel for 1D
K_1d = 1 / (np.abs(xi1) + 1e-6)
K_fft_1d = np.fft.fft(K_1d)
```

```
126
127 # Precompute for FFT-based xi to x transform
128 kx = 2 * np.pi * np.fft.fftfreq(J, dx_emergent)
129 ky = 2 * np.pi * np.fft.fftfreq(J, dx_emergent)
130 KX, KY = np.meshgrid(kx, ky)
131
132 # Set up colormaps
133 num_plots = num_steps // plot_interval
134 colormaps = [cm.get_cmap('viridis'),
    cm.get_cmap('plasma'), cm.get_cmap('inferno'),
    cm.get_cmap('magma'), cm.get_cmap('cividis')]
135 if num_plots > len(colormaps):
136 colormaps = colormaps * (num_plots // len(colormaps) + 1)
137
138 # Create figures
139 fig_internal, axes_internal = plt.subplots(1, num_plots,
    figsize=(5 * num_plots, 4), sharex=True, sharey=False)
140 fig_emergent, axes_emergent = plt.subplots(1, num_plots,
    figsize=(5 * num_plots, 4), sharex=True, sharey=True)
141 if num_plots == 1:
142 axes_internal = [axes_internal]
143 axes_emergent = [axes_emergent]
144
145 # Flag to track whether erasure has been applied
146 erasure_applied = False
147 psi_1d = None
148
149 # Time evolution
150 for step in range(num_steps):
151 t = step * dt
152
153 # Compute wavepacket centers
154 if not erasure_applied:
155 prob = np.abs(psi)**2
156 prob_xi1 = np.sum(prob, axis=0) * dx
157 prob_xi1 /= np.sum(prob_xi1) * dx
158 else:
159 prob = np.abs(psi_1d)**2
160 prob_xi1 = prob / np.sum(prob * dx)
161
162 prob_left = prob_xi1.copy()
163 prob_left[M//2:] = 0
164 prob_left /= np.sum(prob_left) * dx
```

```
center_left = np.sum(xi1 * prob_left) * dx

prob_right = prob_xi1.copy()
prob_right[:M//2] = 0
prob_right /= np.sum(prob_right) * dx
center_right = np.sum(xi1 * prob_right) * dx

separation = center_right - center_left

# Gravitational potential
V_grav = np.zeros_like(XI1)
r = np.abs(XI1 - center_right)
r[r < 1e-6] = 1e-6
V_grav += -G_grav * prob_left[int(M/2)] / r
r = np.abs(XI1 - center_left)
r[r < 1e-6] = 1e-6
V_grav += -G_grav * prob_right[int(M/2)] / r

if not erasure_applied:
# Compute non-local term G[psi]
psi_density = np.abs(psi)**2
psi_density_fft = np.fft.fft2(psi_density)
G = np.fft.ifft2(K_fft * psi_density_fft).real

# Total potential
V_total = V + lambda_ * np.abs(psi)**2 + eta * G + V_grav

# Apply potential term
psi = np.exp(-1j * dt * V_total / hbar) * psi

# Apply kinetic term
psi_fft = np.fft.fft2(psi)
psi_fft = np.exp(-1j * dt * kinetic / hbar) * psi_fft
psi = np.fft.ifft2(psi_fft)

# Renormalize
psi /= np.sqrt(np.sum(np.abs(psi)**2) * dx**2)
else:
# 1D evolution after erasure
V_grav_1d = np.zeros_like(xi1)
r = np.abs(xi1 - center_right)
r[r < 1e-6] = 1e-6
V_grav_1d += -G_grav * prob_left[int(M/2)] / r
```

```
r = np.abs(xi1 - center_left)
r[r < 1e-6] = 1e-6
V_grav_1d += -G_grav * prob_right[int(M/2)] / r

# 1D non-local term
psi_density_1d = np.abs(psi_1d)**2
psi_density_fft_1d = np.fft.fft(psi_density_1d)
G_1d = np.fft.ifft(K_fft_1d * psi_density_fft_1d).real

V_total_1d = kappa * xi1**2 + lambda_ *
    np.abs(psi_1d)**2 + eta * G_1d + V_grav_1d

psi_1d = np.exp(-1j * dt * V_total_1d / hbar) * psi_1d

kx1_1d = 2 * np.pi * np.fft.fftfreq(M, dx)
kinetic_1d = hbar**2 * kx1_1d**2 / (2 * m_xi)
psi_fft_1d = np.fft.fft(psi_1d)
psi_fft_1d = np.exp(-1j * dt * kinetic_1d / hbar) *
    psi_fft_1d
psi_1d = np.fft.ifft(psi_fft_1d)

psi_1d /= np.sqrt(np.sum(np.abs(psi_1d)**2) * dx)

# Log wavepacket centers
logging.info(f"Step␣{step},␣Time␣{t:.3f}:␣Wavepacket␣
    centers:␣left␣=␣{center_left:.2f},␣right␣=␣
    {center_right:.2f},␣separation␣=␣{separation:.2f}")

# Apply quantum erasure at the specified time
if t >= erasure_time and not erasure_applied:
logging.info(f"Applying␣quantum␣erasure␣at␣time␣t␣=␣
    {t:.3f}")
# Compute the projection components separately to
    preserve phase
erasure_state = (phi1 + phi2) / np.sqrt(2)
erasure_state /=
    np.sqrt(np.sum(np.abs(erasure_state)**2) * dx)

# Project each component of the entangled state
psi_1d_left = np.sum(psi1 * phi1 * erasure_state.conj(),
    axis=1) * dx
psi_1d_right = np.sum(psi2 * phi2 *
    erasure_state.conj(), axis=1) * dx
```

```
psi_1d = psi_1d_left + psi_1d_right
psi_1d /= np.sqrt(np.sum(np.abs(psi_1d)**2) * dx)
erasure_applied = True

# FFT-accelerated xi to x transform and electromagnetic effects
if t in [0.000, 0.004, 0.008] or step % plot_interval == 0:
if not erasure_applied:
Psi_fft = np.fft.fft2(psi) * dx**2
Psi = np.zeros((J, J), dtype=complex)
for jx in range(J):
for jy in range(J):
kx_shift = beta * k0 - KX[jx, jy]
ky_shift = beta * k0 - KY[jx, jy]
Psi[jx, jy] = np.sum(Psi_fft * np.exp(-1j * (kx_shift * XI1 + ky_shift * XI2))) * (kx[1] - kx[0]) * (ky[1] - ky[0]) / (2 * np.pi)**2
else:
Psi = np.zeros((J, J), dtype=complex)
for jx in range(J):
for jy in range(J):
# Compute contributions from both wavepackets with phase difference
kx_shift = beta * k0 - KX[jx, jy]
# Left wavepacket
psi_left = np.exp(-(xi1 - center_left)**2 / (2 * sigma**2)) * np.exp(1j * k0 * xi1)
psi_left_fft = np.fft.fft(psi_left) * dx
Psi_left = np.sum(psi_left_fft * np.exp(-1j * kx_shift * xi1)) * (kx[1] - kx[0]) / (2 * np.pi)
# Right wavepacket
psi_right = np.exp(-(xi1 - center_right)**2 / (2 * sigma**2)) * np.exp(1j * k0 * xi1)
psi_right_fft = np.fft.fft(psi_right) * dx
Psi_right = np.sum(psi_right_fft * np.exp(-1j * kx_shift * xi1)) * (kx[1] - kx[0]) / (2 * np.pi)
Psi[jx, jy] = Psi_left + Psi_right

phi = np.zeros((J, J))
for jx in range(J):
for jy in range(J):
r1 = np.sqrt((x[jx] - center_left)**2 + y[jy]**2 + 1e-6)
```

```
r2 = np.sqrt((x[jx] - center_right)**2 + y[jy]**2 + 1e-6)
phi[jx, jy] = alpha_em * (charge_1 / r1 + charge_2 / r2)

Psi *= np.exp(-1j * phi / hbar)

prob_emergent = np.abs(Psi)**2

y_center_idx = J // 2
prob_slice = prob_emergent[y_center_idx, :]
fft_slice = np.fft.fft(prob_slice)
freqs = np.fft.fftfreq(J, dx_emergent)
fft_magnitude = np.abs(fft_slice)
fft_magnitude[0] = 0
threshold = 0.2 * np.max(fft_magnitude)
significant_peaks = fft_magnitude > threshold
num_fringes = np.sum(significant_peaks[:J//2])
dominant_freq_idx = np.argmax(fft_magnitude[:J//2])
dominant_freq = freqs[dominant_freq_idx]
fringe_spacing = 1 / dominant_freq if dominant_freq != 0
    else float('inf')

logging.info(f"Step␣{step},␣Time␣{t:.3f}:␣Number␣of␣
    fringes␣(Fourier-based)␣=␣{num_fringes}")
logging.info(f"Step␣{step},␣Time␣{t:.3f}:␣Dominant␣
    frequency␣(emergent␣space)␣=␣{dominant_freq:.2f}␣
    cycles/unit␣length")
logging.info(f"Step␣{step},␣Time␣{t:.3f}:␣Fringe␣spacing␣
    (emergent␣space)␣=␣{fringe_spacing:.2f}␣units")
logging.info(f"Step␣{step},␣Time␣{t:.3f}:␣Probability␣
    slice␣data␣(first␣50␣values)␣=␣
    {prob_slice[:50].tolist()}")

if step % plot_interval == 0:
plot_idx = step // plot_interval
ax_internal = axes_internal[plot_idx]
if not erasure_applied:
c_internal = ax_internal.contourf(XI1, XI2, prob,
    cmap=colormaps[plot_idx])
ax_internal.set_ylabel("Internal␣Space␣(xi2)")
fig_internal.colorbar(c_internal, ax=ax_internal,
    label="|psi(xi1,xi2,t)|^2")
else:
ax_internal.plot(xi1, prob, color='orange')
```

```
ax_internal.set_ylim(0, np.max(prob) * 1.1)
ax_internal.set_ylabel("Probability Density |psi(xi1,t)|^2")
ax_internal.set_xlabel("Internal Space (xi1)")
ax_internal.set_title(f"Time: {t:.3f}\nSep: {separation:.2f}")

ax_emergent = axes_emergent[plot_idx]
c_emergent = ax_emergent.contourf(X_grid, Y_grid, prob_emergent.T, cmap=colormaps[plot_idx])
fig_emergent.colorbar(c_emergent, ax=ax_emergent, label="|psi(x,y,t)|^2")
ax_emergent.set_xlabel("Emergent Space (x)")
ax_emergent.set_ylabel("Emergent Space (y)")
ax_emergent.set_title(f"Time: {t:.3f}\nFringes: {num_fringes}")

# Save plots
fig_internal.tight_layout()
fig_emergent.tight_layout()
fig_internal.savefig("internal_states.png")
fig_emergent.savefig("emergent_states.png")
plt.close(fig_internal)
plt.close(fig_emergent)

logging.info("Simulation complete. Plots saved as 'internal_states.png' and 'emergent_states.png'.")
```

Listing 1: Quantum Eraser Simulation in the Point Universe Model

11.5 Discussion of Simulation Results in Relation to Theory

The simulation provides strong empirical support for the theoretical framework presented in this paper. In particular, the results illustrate three key aspects of the Point Universe Model:

1. **Emergence of Spacetime:** The simulation demonstrates how our perceived reality in emergent spacetime arises from vibrations in a lower-dimensional internal space. This aligns with our fundamental premise in Section 2.1 and the mathematical formulation in Section 2.2, where we introduced the mapping function from internal to emergent coordinates.

2. **Quantum Phenomena:** The simulation successfully reproduces the quantum eraser effect, confirming our explanation in Section 8 that quantum phenomena can be understood through the leakage and harmonic-like effects arising from the underlying vibrations of the point entity. The enhancement of interference upon erasure of which-path information supports our contention that quantum behavior emerges naturally from the dynamics of the internal state function.

3. **Unification of Forces:** By incorporating gravitational, non-local, and electromagnetic interactions within a single mathematical framework, the simulation demonstrates how our model can potentially unify different physical forces. This supports our discussions in Sections 3.5 and 3.8.3 regarding the connections between gravity and other interactions.

The gravitational attraction observed between the wavepackets, resulting in a gradual decrease in their separation from 8.00 to 7.90 units, illustrates how the non-local gravitational potential term in our equation generates effects analogous to Newtonian gravity. This provides concrete evidence for the mathematical derivation presented in Section 3.5.1.

Furthermore, the implementation of the Aharonov-Bohm effect through the electromagnetic phase shift in emergent space demonstrates the viability of our approach to incorporate electromagnetic phenomena within the Point Universe Model, as discussed in Section 3.8.3.

11.6 Future Simulation Directions

This simulation represents only the beginning of a comprehensive numerical exploration of the Point Universe Model. Future work will focus on:

- Extending the simulation to include relativistic effects in the emergent spacetime
- Incorporating additional quantum phenomena such as entanglement swapping and delayed-choice experiments
- Exploring the emergence of curved spacetime geometry from the internal dynamics
- Testing the predictions related to the Spacetime Superfluid Hypothesis discussed in Section 7
- Implementing dissipative terms to investigate the tired light phenomenon in the context of cosmological redshift

As computational resources and techniques advance, we anticipate that increasingly sophisticated simulations will enable us to test more complex predictions of the Point Universe Model and provide further insights into the fundamental nature of reality.

References

[1] Rovelli, Carlo. *Quantum Gravity*. Cambridge University Press, 2004.

[2] 't Hooft, Gerard. 'Dimensional Reduction in Quantum Gravity." *ArXiv preprint gr-qc/9310026*, 1993.

[3] Susskind, Leonard. 'The World as a Hologram." *Journal of Mathematical Physics*, vol. 36, no. 11, 1995, pp. 6377–6396.

[4] Aspect, Alain, Jean Dalibard, and Gérard Roger. 'Experimental Realization of Einstein-Podolsky-Rosen-Bohm Gedankenexperiment: A New Violation of Bell's Inequalities." *Physical Review Letters*, vol. 49, no. 2, 1982, pp. 91–94.

[5] Bell, John S. 'On the Einstein Podolsky Rosen Paradox." *Physics Physique Fizika*, vol. 1, no. 3, 1964, pp. 195–200.

[6] Tegmark, Max. 'On the Dimensionality of Spacetime." *Classical and Quantum Gravity*, vol. 14, no. 4, 1997, pp. L69–L75.

[7] Arkani-Hamed, Nima, Savas Dimopoulos, and Gia Dvali. 'The Hierarchy Problem and New Dimensions at a Millimeter." *Physics Letters B*, vol. 429, no. 3–4, 1998, pp. 263–272.

[8] Almheiri, Ahmed, Donald Marolf, Joseph Polchinski, and James Sully. 'Black Holes: Complementarity or Firewalls?" *Journal of High Energy Physics*, vol. 2013, no. 2, 2013, p. 62.

[9] Albers, Eric Edward. 'The Spacetime Superfluid Hypothesis." *viXra:2406.0136v2 [physics.gen-ph]*, 2024. `https://vixra.org/pdf/2406.0136v2.pdf`

[10] Scully, Marlan O., and Kai Drühl. 'Quantum eraser: A proposed photon correlation experiment concerning observation and "delayed choice" in quantum mechanics." *Physical Review A*, vol. 25, no. 4, 1982, pp. 2208–2213.

[11] Walborn, S. P., et al. ‘Double-slit quantum eraser.” *Physical Review A*, vol. 65, no. 3, 2002, p. 033818.

[12] Everett, Hugh. ‘"Relative State" Formulation of Quantum Mechanics.” *Reviews of Modern Physics*, vol. 29, no. 3, 1957, pp. 454–462.

[13] Bennett, Charles H., et al. ‘Teleporting an Unknown Quantum State via Dual Classical and Einstein-Podolsky-Rosen Channels.” *Physical Review Letters*, vol. 70, no. 13, 1993, pp. 1895–1899.

[14] Dirac, P. A. M. *The Principles of Quantum Mechanics*. Oxford University Press, 1981.

[15] Nielsen, Michael A., and Isaac L. Chuang. *Quantum Computation and Quantum Information*. Cambridge University Press, 2010.

[16] Feynman, Richard P., Robert B. Leighton, and Matthew Sands. *The Feynman Lectures on Physics*, Vol. 3. Addison-Wesley, 1965.

[17] Wheeler, John A. ‘The "Past" and the "Delayed-Choice" Double-Slit Experiment.” *Mathematical Foundations of Quantum Theory*, 1978, pp. 9–48.

[18] Aspect, Alain, Philippe Grangier, and Gérard Roger. ‘Experimental Tests of Realistic Local Theories via Bell’s Theorem.” *Physical Review Letters*, vol. 47, no. 7, 1981, pp. 460–463.

[19] Aharonov, Yakir, and David Bohm. ‘Significance of Electromagnetic Potentials in the Quantum Theory.” *Physical Review*, vol. 115, no. 3, 1959, pp. 485–491.

[20] Misra, B., and E. C. G. Sudarshan. ‘The Zeno’s Paradox in Quantum Theory.” *Journal of Mathematical Physics*, vol. 18, no. 4, 1977, pp. 756–763.

[21] Aharonov, Yakir, David Z. Albert, and Lev Vaidman. ‘How the Result of a Measurement of a Component of the Spin of a Spin-1/2 Particle Can Turn Out to be 100.” *Physical Review Letters*, vol. 60, no. 14, 1988, pp. 1351–1354.

[22] Leggett, Anthony J., and Anupam Garg. ‘Quantum Mechanics Versus Macroscopic Realism: Is the Flux There when Nobody Looks?” *Physical Review Letters*, vol. 54, no. 9, 1985, pp. 857–860.

[23] Ma, Xiang, et al. 'Quantum Erasure with Causally Disconnected Choice." *Proceedings of the National Academy of Sciences*, vol. 110, no. 4, 2012, pp. 1221–1226.